



The Thomas Jefferson National Accelerator Facility
Theory Group Preprint Series

JLAB-THY-98-09
WM-98-102

QCD Evolution Equations: Numerical Algorithms from the Laguerre Expansion

Additional copies are available from the authors.

The Southeastern Universities Research Association (SURA) operates the Thomas Jefferson National Accelerator Facility for the United States Department of Energy under contract DE-AC05-84ER40150.

Claudio Coriano^{**1} and Cetin Savkli^{**1,2}

^{**} Theory Group, Jefferson Lab, Newport News, VA 23606, USA

¹ Dept. of Physics, College of William and Mary, Williamsburg, VA, 23187

Abstract

A complete numerical implementation, in both singlet and non-singlet sectors, of a very elegant method to solve the QCD Evolution equations, due to Furmanski and Petronzio, is presented. The algorithm is directly implemented in x -space by a Laguerre expansion of the parton distributions. All the leading-twist distributions are evolved: longitudinally polarised, transversely polarised and unpolarised, to NLO accuracy. The expansion is optimal at finite x , up to reasonably small x -values ($x \approx 10^{-3}$), below which the convergence of the expansion slows down. The polarized evolution is smoother, due to the less singular structure of the anomalous dimensions at small- x . In the region of fast convergence, which covers most of the usual perturbative applications, high numerical accuracy is achieved by expanding over a set of approximately 30 polynomials, with a very modest running time.

DISCLAIMER

This report was prepared as an account of work sponsored by the United States government. Neither the United States nor the United States Department of Energy, nor any of their employees, makes any warranty, expressed or implied, or assumes any legal liability or responsibility for the accuracy, completeness, or usefulness of any information, apparatus, product, or process disclosed, or represents that its use would not infringe privately owned rights. Reference herein to any specific commercial product, process, or service by trade name, mark, manufacturer, or otherwise, does not necessarily constitute or imply its endorsement, recommendation, or favoring by the United States government or any agency thereof. The views and opinions of authors expressed herein do not necessarily state or reflect those of the United States government or any agency thereof.

¹E-mail address: coriano@jlab2.jlab.org

²csavkli@physics.wm.edu

Program Summary

Title of the Programs: nsunpol, anunpol, nslong, slong, trans

Computer:

Operating system: Unix

Programming language used: FORTRAN 77

Peripherals used: Laser Printer

Number of lines in distributed program, including test data, etc.:

Keywords: Structure function, polarized parton distribution, Q^2 evolution, Laguerre method, numerical solution.

Nature of physical problem:

The programs provided here solve the DGLAP evolution equations, with next-to-leading order α_s effects taken to account, for unpolarized, longitudinally polarized and transversely polarized parton distributions.

Method of solution:

The method developed by Furmanski and Petronzio is used. The kernel $P(x)$ of the DGLAP integrodifferential equations and the evolution operators $E(t, x)$ are expanded in Laguerre polynomials.

Restrictions of the program:

Typical running time:

About 5 seconds for the transverse polarization case and 30 minutes for longitudinal polarization and for the unpolarized.

LONG WRITE-UP

1 Introduction

The study of the spin structure of the proton is a fascinating aspect of the theory of the strong interactions. Parton distributions in the nucleon tell us about the structure of fundamental observables such as spin, parton densities and correlations among partons, in a light-cone framework. In a second quantized theory they emerge as matrix elements of nonlocal operators at light-like separations. At low energy they can be described by

valence quark models and the impact of the QCD evolution (or Renormalization Group Evolution, RGE) on the shape of these distributions can be performed within the parton model.

It has become more and more common in the high energy literature to describe the evolution of parton distributions by starting from a low energy input.

There is widespread interest in the analysis of the effect of the QCD evolution especially for those leading twist distributions (such as the transverse spin distribution) which have not yet been measured. For instance, in ref. [5], the authors analyze the impact of the evolution on transverse spin distributions derived at low Q from the Isgur-Karl quark model [7], and these predictions can be used directly -at very high energy- for other predictions, such as in the study of the transverse spin dependence of the Drell-Yan process. A similar analysis can be done for the chiral quark model [6].

On the numerical side, various methods have been presented in the literature [10] which all try to solve the DGLAP equations by iterating the evolution over infinitesimal steps in the fractional momentum x . Another technique is based on the use of Mellin moments and on their inversion. In general, moments are equivalent to finite -rather than infinitesimal- discretizations of the integro-differential equations. In the case of the Mellin moments the inversion (to x -space) is the real difficult and time consuming part of the method.

A different, and very elegant implementation of methods based on finite discretizations of RGE's for QCD was formulated long ago by Furmanski and Petronzio [2]. Their method uses the Laguerre expansion of the initial distributions and of the kernel of the evolution equations arrested to an arbitrary order n . The algorithm that they provide defines the structure of the moments recursively in terms of some initial conditions. In the non-singlet sector there have been attempts to apply the method both to leading and to next to leading order [18, 11], and to leading order in the singlet sector as well [18]. However, a complete implementation and numerical documentation of this algorithm is still missing. We also mention that our interest in this method has aroused from our search for the numerical implementations of more involved evolutions equations, such as those describing the dynamics of Compton scattering in the deeply virtual limit (DVCS) [9]. In this latter case, the RGE evolution is a continuous interpolation between 2 limits: the DGLAP (or Altarelli Parisi) evolution and the Efremov-Radyushkin-Brodsky-Lepage evolution (ERBL) [8]. We believe that a complete numerical understanding of these "non-diagonal" RGE's and their robust numerical implementation requires finite step integrations. We hope to get back to this issue in the near future, and for the rest of this paper just focus on the usual DGLAP evolution. Here we have implemented the evolution of all the leading twist parton distributions, using the kernels calculated by various authors [2, 3, 13, 14]. A complete list of these kernels can be found in the Appendix.

2 The Laguerre expansion

The Laguerre method for the numerical solution of the evolution equations is due to Furmanski and Petronzio. In this section we briefly outline the method, which is fast converging at intermediate values of x and any Q^2 value. At very small- x (approx 10^{-3}), the Laguerre expansion suffers from numerical instabilities, due to the growth of the moments. We start by defining our notation and other conventions.

The two-loop running of the coupling constant is defined by

$$\frac{\alpha(Q_0^2)}{2\pi} = \frac{2}{\beta_0} \frac{1}{\ln(Q^2/\Lambda^2)} \left(1 - \frac{\beta_1}{\beta_0} \frac{\ln \ln(Q^2/\Lambda^2)}{\ln(Q^2/\Lambda^2)} + O\left(\frac{1}{\ln^2(Q^2/\Lambda^2)}\right) \right). \quad (1)$$

where

$$\begin{aligned} \beta_0 &= \frac{11}{3}C_G - \frac{4}{3}T_R n_f \\ \beta_1 &= \frac{34}{3}C_G^2 - \frac{10}{3}C_G n_f - 2C_F n_f \end{aligned} \quad (2)$$

where

$$C_G = N, \quad C_F = \frac{N^2 - 1}{2N}, \quad T_R = \frac{1}{2} \quad (3)$$

and N is the number of colours.

The solution for the running coupling is given by

$$\alpha(t) = \frac{\alpha(0)}{2\pi} e^{-\beta_0 t/2\pi} \quad (4)$$

with $\alpha(Q_0^2) \equiv \alpha(0)$ The evolution equations are (generically) of the form

$$\begin{aligned} Q^2 \frac{d}{dQ^2} q_i^{(-)}(x, Q^2) &= \frac{\alpha(Q^2)}{2\pi} P_{(-)}(x, \alpha(Q^2)) \otimes q_i^{(-)}(x, Q^2) \\ Q^2 \frac{d}{dQ^2} \chi_i(x, Q^2) &= \frac{\alpha(Q^2)}{2\pi} P_{(-)}(x, \alpha(Q^2)) \otimes \chi_i(x, Q^2) \end{aligned} \quad (5)$$

with

$$\chi_i(x, Q^2) = q_i^{(+)}(x, Q^2) - \frac{1}{n_F} q_i^{(+)}(x, Q^2) \quad (6)$$

for the non-singlet distributions and

$$Q^2 \frac{d}{dQ^2} \begin{pmatrix} q^{(+)}(x, Q^2) \\ G(x, Q^2) \end{pmatrix} = \begin{pmatrix} P_{qq}(x, Q^2) & P_{qg}(x, Q^2) \\ P_{gq}(x, Q^2) & P_{gg}(x, Q^2) \end{pmatrix} \otimes \begin{pmatrix} q^{(+)}(x, Q^2) \\ G(x, Q^2) \end{pmatrix} \quad (7)$$

for the singlet sector.

We have defined, as usual

$$q_i^{(-)} = q_i - \bar{q}_i, \quad q_i^{(+)} = q_i + \bar{q}_i, \quad q^{(+)} \equiv \Sigma = \sum_{i=1}^{n_f} q_i^{(+)} \quad (8)$$

We introduce the evolution variable

$$t = -\frac{2}{\beta_0} \ln \frac{\alpha(Q^2)}{\alpha(Q_0^2)} \quad (9)$$

which replaces Q^2 .

The evolution equations are then rewritten in the form

$$\frac{d}{dt} q_i^{(-)}(t, x) = \left(P^{(0)}(x) + \frac{\alpha(t)}{2\pi} R_{(-)}(x) + \dots \right) \otimes q_i^{(-)}(t, x) \quad (10)$$

$$Q^2 \frac{d}{dt} \chi_i(x, Q^2) = \left(P^{(0)}(x) + \frac{\alpha(t)}{2\pi} R_{(+)}(x) \right) \otimes \chi_i(x, Q^2), \quad (11)$$

$$\frac{d}{dt} \begin{pmatrix} q^{(+)}(t, x) \\ G(x, t) \end{pmatrix} = \left(P^{(0)}(x) + \frac{\alpha(t)}{2\pi} R(x) + \dots \right) \otimes \begin{pmatrix} q^{(+)}(t, x) \\ G(x, t) \end{pmatrix}. \quad (12)$$

In the new variable t , the kernels of the evolution take the form

$$\begin{aligned} R_{(\pm)}(x) &= P_{(\pm)}^{(1)}(x) - \frac{\beta_1}{2\beta_0} P_V^{(0)}(x) \\ R(x) &= P^{(1)}(x) - \frac{\beta_1}{2\beta_0} P^{(0)}(x). \end{aligned} \quad (13)$$

Equations (10) and (11) are solved independently for the variables $q_i^{(-)}$ and χ_i respectively. Finally, the solution $q^{(+)}$ of eq. (12) (or the singlet equation) is substituted into χ_i in order to obtain $q_i^{(+)}$.

The equations can be written down in terms of two singlet evolution operators $E_{\pm}(t, x)$ and initial conditions $\bar{q}_{\pm}(x, t=0) \equiv \bar{q}_{\pm}(x)$ as

$$\frac{d}{dt} E_{\pm} = P_{\pm} \otimes E_{\pm}, \quad (14)$$

whose solutions are given by

$$\begin{aligned} q_i^{(-)}(t, x) &= E_{(-)} \otimes \bar{q}_i^{(-)} \\ \chi_i(t, x) &= E_{(+)} \otimes \bar{\chi}_i(x). \end{aligned} \quad (15)$$

The singlet evolution for the matrix operator $E(t, x)$

$$\begin{pmatrix} E_{FF} & E_{FG} \\ E_{GF} & E_{GG} \end{pmatrix} \quad (16)$$

$$\frac{dE}{dt} = P \otimes E \quad (17)$$

is solved similarly as

$$\begin{pmatrix} q^{(+)}(t, x) \\ G(t, x) \end{pmatrix} = E(t, x) \otimes \begin{pmatrix} \tilde{q}^{(+)}(x) \\ \tilde{G}(x) \end{pmatrix}. \quad (18)$$

$$(19)$$

The method of Furmanski and Petronzio requires an expansion of the splitting functions and of the parton distributions in the basis of the Laguerre polynomials

$$L_n(y) = \sum_{k=0}^n \binom{n}{k} (-1)^k \frac{y^k}{k!} \quad (20)$$

which satisfies the property of closure under a convolution

$$L_n(y) \otimes L_m(y) = L_{n+m}(y) - L_{n+m+1}(y). \quad (21)$$

In order to improve the small- x behaviour of the algorithm, from now on, the evolution is applied to the modified kernel $xP(x)$, which, for simplicity, is still denoted as in all the equations above, i.e. by $P(x)$. At a second step, the $0 < x < 1$ interval is mapped into an infinite interval $0 < y < \infty$ by a change of variable $x = e^{-y}$ and all the integrations are performed in this last interval.

We start from the non-singlet case by defining the Laguerre expansion of the kernels and the corresponding (Laguerre) moments to lowest order

$$\begin{aligned} P_V^{(0)}(y) &= \sum_{n=0}^{\infty} P_n^{(0)} L_n(y), \\ P_n^{(0)} &= \int_0^{\infty} dy e^{-y} L_n(y) P^{(0)}(y) \end{aligned} \quad (22)$$

and to NLO

$$R(y) = \sum_{n=0}^{\infty} R_n L_n(y). \quad (23)$$

One defines also the difference of moments

$$\begin{aligned} p_i^{(0)} &= P_i^{(0)} - P_{i-1}^{(0)} \quad (P_{-1}^{(0)} = 0) \\ r_i &= R_i - R_{i-1} \quad R_{-1} = 0. \end{aligned} \quad (24)$$

A similar expansion is set up for the evolution operators $E(t, y)$

$$\begin{aligned} E^{(0)}(t, y) &= \sum_{n=0}^{\infty} E_n^{(0)}(t) L_n(y) \\ E^{(1)}(t, y) &= \sum_{n=0}^{\infty} E_n^{(1)}(t) L_n(y), \end{aligned} \quad (25)$$

where all the information on the t evolution is contained in the moments $E_n(t)$. The solution to NLO is expressed as [4]

$$E_n(t) = E_n^{(0)}(t) - \frac{2}{\beta_0} \frac{\alpha(t) - \alpha(0)}{2\pi} E_n^{(1)}(t), \quad (26)$$

where

$$E_n^{(0)}(t) = e^{P_n^{(0)} t} \sum_{k=0}^n \frac{A_n^{(k)} t^k}{k!} \quad (27)$$

$$E_n^{(1)}(t) = \sum_i^n r_{n-i} E_i^{(0)}(t), \quad (28)$$

$$(29)$$

and the coefficients $A_n^{(k)}$ are determined recursively from the moments of the lowest order kernel $P^{(0)}$

$$\begin{aligned} A_n^{(0)} &= 1 \\ A_n^{(k+1)} &= \sum_{i=k}^{n-1} P_{n-i}^{(0)} A_i^{(k)} \quad (k = 0, 1, 2, \dots, n-1) \end{aligned} \quad (30)$$

In the singlet case one proceeds in a similar way. The solution is expressed in terms of a 2-by-2 matrix operator

$$E^{(0)}(t, y) = \sum_{n=0}^{\infty} E_n^{(0)}(t) L_n(y). \quad (31)$$

The solution (at leading order) is written down in terms of 2 projection matrices and one eigenvalue (λ) of the $P^{(0)}$ (matrix) kernel

$$e_1 = \frac{1}{\lambda} P^{(0)}, \quad e_2 = \frac{1}{\lambda} (-P^{(0)} + \lambda \mathbf{1}), \quad (32)$$

$$(33)$$

where

$$\lambda = -\left(\frac{4}{3}C_F + \frac{2}{3}n_f T_R\right), \quad (34)$$

in the form

$$E_n^{(0)}(t) = \sum_{k=0}^n \frac{t^k}{k!} (A_n^{(k)} + B_n^{(k)} e^{\lambda t}). \quad (35)$$

The recursion relations which allow to build $A_n^{(k)}$ and $B_n^{(k)}$ are solved in two steps as follows. One solves first for two sets of matrices $a_n^{(k)}$ and $b_n^{(k)}$ by the relations

$$\begin{aligned} a_n^{(0)} &= 0 \\ a_n^{(k+1)} &= \lambda e_1 a_n^{(k)} + \sum_{i=k}^{n-1} p_{n-i}^{(0)} a_i^{(k)} \\ b_n^{(0)} &= 0 \\ b_n^{(k+1)} &= -\lambda e_2 b_n^{(k)} + \sum_{i=1}^{n-1} p_{n-i}^{(0)} b_i^{(k)}, \end{aligned} \quad (36)$$

which are used to construct the matrices $A_n^{(0)}$ and $B_n^{(0)}$

$$\begin{aligned} A_n^{(0)} &= e_2 - \frac{1}{\lambda^n} (e_1 a_n^{(n)} - (-1)^n e_2 b_n^{(n)}) \\ B_n^{(0)} &= e_1 + \frac{1}{\lambda^n} (e_1 a_n^{(n)} - (-1)^n e_2 b_n^{(n)}). \end{aligned} \quad (37)$$

$$(38)$$

These matrices are then input in the recursion relations

$$\begin{aligned} A_0^{(0)} &= e_2 & B_0^{(0)} &= e_1 \\ A_n^{(k+1)} &= \lambda e_1 A_n^{(k)} + \sum_{i=k}^{n-1} p_{n-i}^{(0)} A_i^{(k)} \\ B_n^{k+1} &= -\lambda e_2 B_n^{(k)} + \sum_{i=k}^{n-1} p_{n-i}^{(0)} B_i^{(k)} \end{aligned} \quad (39)$$

7

with $n >$) and $k = 0, 1, \dots, n-1$, which generates the coefficients of the matrix-valued operator $E^{(0)}$ (i.e. the leading order solution). The NLO part of the evolution is obtained from

$$E^{(1)}(t, y) = \sum_{n=0}^{\infty} E_n^{(1)}(t) L_n(y), \quad (40)$$

with

$$E_n^{(1)}(t) = \tilde{E}_n^{(1)}(t) - 2\tilde{E}_{n-1}^{(1)}(t) + \tilde{E}_{n-2}^{(1)}(t) \quad (41)$$

where

$$\tilde{E}_n^{(1)}(t) = \int_0^t d\tau e^{-\beta_0 \tau/2} \sum_{ijk} E^{(0)}(t-\tau) R_j E_k^{(0)}(\tau) \delta(n-i-j-k). \quad (42)$$

The expressions of $E^{(0)}$ and $E^{(1)}$ are inserted into eq. (26) thereby providing a complete NLO solution of the singlet sector.

3 The Polarized and the unpolarized evolution

The implementation of the polarized and of the unpolarized evolution is performed in the \overline{MS} scheme, which is by now standard in most of the high energy physics applications. In the unpolarized case, we introduce valence quark distributions $q_V(x, Q_0^2)$ and gluon distributions $G(x, Q_0^2)$ at the input scale Q_0 , together with initial sea distributions $\bar{q}_i(x, Q_0^2)$ taken from the CTEQ parametrization [25]

$$q(x) = A_0 x^{A_1} (1-x)^{A_2} (1+A_3 x^{A_4}). \quad (43)$$

Specifically

$$\begin{aligned} x u_V(x) &= 1.344 x^{0.501} (1-x)^{3.689} [1 + 6.042 x^{0.873}] \\ x d_V(x) &= 0.640 x^{0.501} (1-x)^{4.247} [1 + 2.690 x^{0.333}] \\ x G(x) &= 1.123 x^{-0.206} (1-x)^{4.673} [1 + 4.269 x^{1.508}] \end{aligned} \quad (44)$$

and an asymmetric sea contribution

$$x \bar{q}(x) = \frac{1}{2} [0.255 x^{-0.143} (1-x)^{8.041} (1+6.112x) \mp 0.071 x^{0.501} (1-x)^{8.041}], \quad (45)$$

where the $(-)$ holds for the \bar{u} and the $(+)$ for the \bar{d} flavors. The set accounts for a \bar{u}, \bar{d} flavour asymmetry, and the sea quark contribution is parameterized by

8

$$x\bar{s}(x) = [0.064x^{-0.143}(1-x)^{8.041}(1+6.112x)]. \quad (46)$$

In the polarized case we have chosen the first set of ref. [20] which is of the functional form $ABx^C(1-x)^D(1+Ex+F\sqrt{x})$

$$\begin{aligned} x\Delta u_V &= 0.918 * 1.365 * x^{0.512}(1-x)^{3.96}(1+11.65x-4.6\sqrt{x}) \\ x\Delta d_V &= -0.339 * 3.849x^{0.78}(1-x)^{4.96}(1+7.81x-3.48\sqrt{x}) \\ x\Delta G &= 1.71 * 3.099x^{0.724}(1-x)^{5.71}(1+0.0x+0.0\sqrt{x}). \end{aligned} \quad (47)$$

For the (flavour symmetric) sea contribution we have set $\Delta\bar{u} = \Delta\bar{d} = \Delta\bar{s}$ with

$$\Delta\bar{s} = -0.06 * 18.521x^{0.724}(1-x)^{14.4}(1+4.63x-4.96\sqrt{x}). \quad (48)$$

Notice that the evolution in the \overline{MS} requires some care, depending upon the way the subtraction of the collinear singularities in the coefficient functions (hard scatterings) is performed. The (non singlet) hard scatterings, in fact, do not conserve helicities in the annihilation channels. In a "traditional" \overline{MS} scheme, one has to keep both these helicity violating terms of the coefficient functions and has add to the polarized non-singlet kernels of the Appendix some additional terms proportional to $(1-x)$ to NLO [15, 17, 13] As a result of this, both the singlet and the non-singlet evolution are affected to NLO.

However, one can factorize out of the coefficient functions these spuriuos (helicity-violating) terms and absorb them into the renormalization of the parton distributions. As a result of this procedure, the NLO kernels of the evolution turn out to be exactly those defined in the Appendix and the hard-scatterings are helicity preserving.

4 Q^2 evolution equation for the transverse distribution

The first identification of the transverse spin distribution is due to Ralston and Soper [23] in their study of the factorization formula for the Drell Yan cross section. The parton interpretation of this distribution has been discussed in various papers [16, 24], in which its behaviour as a leading twist behaviour has been pointed out.

It appears in the double transverse spin asymmetry A_{TT} for the Drell Yan process [23, 24]

$$A_{TT} = \frac{\sin^2 \theta \cos 2\phi \sum_i e_i^2 \Delta_T q_i(x_1) \Delta_T \bar{q}_i(x_2)}{1 + \cos^2 \theta \sum_i e_i^2 q_i(x_1) \bar{q}_i(x_2)}. \quad (49)$$

In eq. (49) the angles θ and ϕ are the polar and the azimuthal angles of the momentum of one of the two leptons, measured with respect to the beam (θ) and to the photon

polarization directions (ϕ). The asymmetry disappears if the momenta of the two leptons are both integrated over. In the parton model, $\Delta_T(q)$ is interpreted as the probability of finding a quark with spin polarized along the transverse spin of a transversely polarized proton minus the probability to find it polarized oppositely. This distribution does not couple to gluons and is therefore, purely non-singlet. The LO anomalous dimensions of this distribution have been calculated in [16], while the NLO corrections have been derived by various authors [17], using both the Operator Product Expansion and the method of ref. [12], extended to the polarized case.

Since the gluon don't couple in the evolution, the equation is simply written as

$$\frac{\partial}{\partial \ln Q^2} \Delta_T q_{\pm}(x, Q^2) = \frac{\alpha_s(Q^2)}{2\pi} \Delta_T P_{q\pm}(x) \otimes \Delta_T q_{\pm}(x, Q^2). \quad (50)$$

As in the previous sections, we have set $\Delta_T q_{\pm} = \Delta_T q \pm \Delta_T \bar{q}$.

5 Description of the program

The first step in the calculation is the computation of Laguerre moments -or expansion coefficients- of the kernel which are given by an explicit recursion relation.

The solutions of the integral equations are obtained by first discretizing the integrals in the form

$$\int dq f(q) \rightarrow \sum_{i=1}^n w_i f(q_i), \quad (51)$$

where w_i are integration weights for grid-points q_i . Various sets of Gauss-Legendre grid-points are provided (by the GAUSS and the LEGENDRE subroutines) in the interval $(-1, 1)$. In order to map the grid points and the weights from the interval $(-1, 1)$ to the interval $(0, \infty)$, one can use various mappings. The possible types of mapping provided in the code are

(i) MAPNO=1:

$$y(x) = R_{min} + \frac{(1+x)}{1-x+2/(R_{max}-R_{min})}, \quad (52)$$

(ii) MAPNO=2:

$$y(x) = R_{min} + (R_{max} - R_{min}) * (x+1)/2, \quad (53)$$

(iii) MAPNO=3(Ref. [21, 22]):

$$y(x) = R_{min} + \frac{R_d \tan(\frac{\pi}{4}(1+x))}{1 + \frac{R_d}{R_{max}-R_{min}} \tan(\frac{\pi}{4}(1+x))}, \quad (54)$$

where

$$R_d = \frac{R_{med} - R_{min}}{R_{max} - R_{med}} (R_{max} - R_{min}). \quad (55)$$

Because of its flexibility, we use the tangent mapping. According to the tangent mapping,

$$y(-1) = R_{min}, y(0) = R_{med}, y(1) = R_{max}. \quad (56)$$

Therefore, one can safely control the range (R_{min}, R_{max}) and the distribution (R_{med}) of the grid points. With this discretization procedure, continuous integral equations are transformed into nonsingular matrix equations.

6 Description of input parameters and input distribution

6.1 Input parameters

NF	Number of quark flavors
NGRID	Number of grid points
PLQCD	Λ_{qcd}
Q2I	Initial Q^2
Q2F	Final Q^2
RMIN	Smallest grid point
RMED	Median of grid points
RMAX	The maximum grid point
LN	The highest degree of Laguerre polynomial included
IFLAV	1 u quark
	2 d quark
	2 s quark
MAPNO	1 type-1 mapping
	2 linear mapping
	3 tangent mapping
IALPH	0 leading order (LO) in α_s
	1 next-to-leading order (NLO) in α_s

6.2 Arrays

P(I)	Grid points $y = P(I)$, where $RMIN < P(I) < RMAX$
WP(I)	Weights
PT(I)	Grid points $t = PT(I)$, where $0 < t < T = -2/\beta_0 \ln(\alpha_s(q^2)/\alpha_s(q_0^2))$
WT(I)	Weights
PN(LN,IE,JE)	elements of the LN'th Laguerre moment of LO kernel $[P]_{2 \times 2}$
RN(LN,IE,JE)	elements of the LN'th Laguerre moment of NLO kernel $[R]_{2 \times 2}$
SPN(I,IE,JE)	PN(I,IE,JE)- PN(I-1,IE,JE)
E1(J,K)	PN(0,J,K)/ λ
E2(J,K)	-PN(0,J,K)/ λ
SA(K,N,IE,JE)	$[a_n^k]_{2 \times 2}$
SB(K,N,IE,JE)	$[b_n^k]_{2 \times 2}$
A(K,N,IE,JE)	$[A_n^k]_{2 \times 2}$
B(K,N,IE,JE)	$[B_n^k]_{2 \times 2}$
ENT(I,IE,JE)	$[E_n(t)]_{2 \times 2}$
PHI0(Y,IE)	Initial distributions $x\Delta\Sigma_0, x\Delta G_0$ respectively for $IE = 1, 2$
PHI0N(N,IE)	Laguerre moments of initial distribution.
PHIT(I,IE)	Evolved distributions $x\Delta\Sigma, x\Delta G$ respectively for $IE = 1, 2$

The codes provided are stored in three directories named after the polarization types; namely transverse, longitudinal and unpolarized. In each directory there are executable files that can be used to compile the fortran codes (executable file "comp") and run them (executable file "run"). The transverse polarization case is the simplest. For transverse polarization one has only the nonsinglet equation. In the longitudinally polarized and unpolarized cases both singlet and nonsinglet equations are solved. The solutions of the singlet and nonsinglet equations are provided by separate codes. For the longitudinally polarized case the nonsinglet equation is solved by "nslong.f", while the singlet equation is solved by "snlong.f". Both codes use the same input file, which is called "INPUT". Nonsinglet and singlet equations work in coordination with each other. Upon execution of the "run" command, first the nonsinglet equation is solved, and the output is written into data files. Next the nonsinglet equation is solved. The data produced by the solution of the singlet equation is read by the code which solves the nonsinglet equation. The user is expected to prepare the "INPUT" file, compile the codes by using the command "comp" and then run them using the command "run". The procedure for the unpolarized case is the same, with the only difference being the names of the files which are "nsunpol.f" and "snunpol.f". Next, we give the detailed descriptions of the programs "sn*.f"

7 SNLONG and SNUNPOL

Since the only difference between these programs are the kernels and the initial conditions, the explanations provided below equally apply to both.

7.1 Main Program

The main program starts by calling the INPUT subroutine. This subroutine reads 12 input parameters described in Table 6.1. Next, the grid points and the weights are calculated by calling the subroutine GAUS, and they are mapped into the desired interval. The mapping is done by the MAP subroutine.

Then, in order to calculate the Laguerre moments of the kernel and input distributions, the subroutine XPL is called. The factors A_n^* , B_n^* which are used in the construction of the leading order evolution operator E_n^0 are calculated in a subroutine called XBKN. In the next step, the XEN subroutine is called to calculate the evolution operator E_n . Finally, the evolution of the initial distribution is performed in the VQD subroutine. The results for the evolved distributions $\Delta\Sigma(x)$, and $\Delta G(x)$ are written, respectively, into the files "dltsig.dat", and "dltglu.dat". Later, the result for the Σ distribution is read by the program that solves the nonsinglet equation.

7.2 Subroutine INPUT

In this subroutine 12 input parameters are read. In addition to reading these parameters, various constants to be used throughout the program are also defined in the INPUT subroutine. These constants are $PLQCD = \lambda_{QCD}$, $PI = \pi$, $Z3 = \zeta_3$, CF , CG , CA , TR , $BT0 = \beta_0$, $BT1 = \beta_1$, $T = -2/\beta_0 \ln(\alpha_s(q^2)/\alpha_s(q_0^2))$, and $XLMBD = \lambda$.

7.3 Subroutine XPL

In this subroutine we calculate the Laguerre moments of the initial distributions $PHI0(Y,IE)$ and kernels P_0 and $R = P_1 - \beta_1/(2\beta_0)P_0$. In $PHI0(Y,IE)$,

$$Y = \ln(1/X) \equiv P(J), \quad (1)$$

and the IE index is used to label the initial distributions for $x\Delta\Sigma(x)$ (IE=1), and $x\Delta G(x)$ (IE=2). We use the variable $Y = [0, \text{inf})$ rather than $X = [0, 1]$ in calculating the Laguerre moments. The results for the Laguerre moments of the initial distributions are stored in $PHI0N(I,IE)$ where $IE = 1, 2$ corresponds to the Laguerre moments of $x\Delta\Sigma$, $x\Delta G$ respectively, and I refers to the order of Laguerre moments. In order to calculate the Laguerre moments of the kernel, we express it in the following form

$$P = P_r + \frac{P_s}{(1-x)_+} + P_d\delta(1-x). \quad (2)$$

The singular part P_s is regulated according to the "+" regularization prescription, while the regular part P_r is directly integrated. The delta function part requires no numerical integration. Therefore, the contribution of this piece is trivially added after performing the numerical integrals for P_r and P_s . The kernels are stored in the arrays $P0R(Y,IE,JE)$, $P0S(Y,IE,JE)$, $P1R(Y,IE,JE)$, $P1S(Y,IE,JE)$, where "R" and "S" stand for the "regular"

and "singular" parts of the kernels, and $IE = 1, 2$, $JE = 1, 2$ are matrix indices. According to our convention, the distributions are introduced by defining 2×1 vector array as $(x\Delta\Sigma, x\Delta G)$. In this subroutine we also define the arrays $SPN(I,IE,JE)$, $E1(J,K)$ and $E2(J,K)$.

7.4 Subroutine XBKN

In this subroutine we construct the arrays $SA(K,N,IE,JE)$, $SB(K,N,IE,JE)$, $A(K,N,IE,JE)$, $B(K,N,IE,JE)$ using nested loops.

7.5 Subroutine XEN

This is the subroutine where the Laguerre moments of the evolution operator, $ENT(N,IE,JE)$, are constructed. In this subroutine the functions $E0N(N,T,IE,JE)$ and $E1N(N,T,IE,JE)$ are called. These functions represent the 0th and 1st order contributions to the Laguerre moments.

7.6 Function E0N(N,T,IE,JE)

Calculates $E0N(N,T,IE,JE)$ using the previously calculated $A(K,N,IE,JE)$, and $B(K,N,IE,JE)$ arrays. Notice that we have defined $E0N(N,T,IE,JE)$ as a function rather than a subroutine. The reason for this is the following: $E0N(N,XT,IE,JE)$ appears inside an integral in the calculation of $E1N(N,T,IE,JE)$, where $XT(0 < XT < T)$ is the integration variable. Therefore, one needs to know $E0N$ for all possible values of XT .

7.7 Function E1N(N,T,IE,JE)

Calculates $E1N$. The set of grid points for the XT integral is $PT(I)$, and the weights are $WT(I)$. The grid points, which were determined in the main program using the Gauss-Legendre subroutines, are chosen such that $0 < PT(I) < T$.

7.8 Subroutine VQD

Evaluates the final result $PHIT(I,IE)$ for evolved distributions. Here, "I" represents the x (Bjorken) value, where $x = e^I - P(I)$, and IE as usual refers to two different parton distributions, that is $PHIT(I, 1) = xG(x)$, and $PHIT(I, 2) = x\Sigma(x)$ (IE=2).

7.9 Functions XLAG, FCTRL, S2, S1, ST

$XLAG(N,Y)$ computes the Laguerre polynomial of order N at Y. $FCTRL(N)$ computes N!. The result is given in double precision. $S2(X)$ and $S1(x)$ are respectively the functions $S_1(x)$, and $S_2(x)$. $ST(x)$ represents $\tilde{S}(x)$.

7.10 Other functions

We also define various simple functions which are used throughout the program. $ALPHAS(Q^2)$ is $\alpha_s(Q^2)$. $GS(X,A,B,C,D,E,F)$ is the Gehrman-Stirling ansatz "A" [20] for the polarized parton distributions. In addition, for convenience in typing in the kernel for longitudinal parton distributions, we define $PF(X)$, $PGS(X)$, $PGR(X)$, $PNFS(X)$, $PNFR(X)$, $PA(X)$, $FQQ(X)$, $F1QG(X)$, $F2QG(X)$, $F1GQ(X)$, $F2GQ(X)$, $F3GQ(X)$, $F1GGS(X)$, $F1GGR(X)$, $F2GG(X)$, $F3GGS(X)$, $F3GGR(X)$.

7.11 subroutines GAUSS, LEGENDRE and MAP

The $LEGEND(X,L,PSUBL)$ subroutine computes Legendre polynomials of argument x from 0 to order L . The $GAUS(Y,WY,N)$ subroutine determines N gaussian points (in the vector Y) and N weights (in the vector WY). For this routine N must be even and not greater than 100. Since the points and weights are symmetric around zero, only half are stored. The original version of this subroutine was written by S. Cotanch [19], at the Univ. of Pittsburgh in the years 1974-75. The $MAP(Y,WY,N,MTYPE,RMIN,RMAX,RMED)$ subroutine maps the initial set of N grid points $Y(I)$ and weights $WY(I)$ to the desired interval ($RMIN,RMAX$). As explained in detail earlier, the mapping type $MTYPE=3$ allows one to control the median ($RMED$) of the distribution. For the Y variable that we use in calculating the Laguerre moments, we have used $RMIN=0.0D0$, $RMAX=1.0D2$, and $RMED=5.0d0$ Since the Laguerre moment integrals are damped by exponential factors e^{-Y} , $RMAX=1.0D2$ was a large enough cutoff for the integral.

8 NSLONG and NSUNPOL

The structure of the codes $NSLONG$ and $NSUNPOL$ are the same as that of $SNLONG$ and $SNUNPOL$. All subroutine names and their functions are identical. The only major difference comes from the fact that in the nonsinglet case one no longer has a matrix equation. Rather, there are two uncoupled equations. The nonsinglet codes read the $x\Sigma(x)$ results which are produced by the singlet codes.

9 Running the code

In order to get reliable results for $0.001 < x < 1$ we have used approximately 30 Laguerre polynomials. The number of grid points used was $N \approx 60$. The nonsinglet codes run in about 1 minute. The singlet and nonsinglet codes together run in about 20 minutes. At very small x ($x < 0.001$) the Laguerre polynomials diverge, and therefore they are not a convenient basis to use in the very small x region. However, for $0.001 < x < 1$, the results are stable for a reasonable number of Laguerre polynomials.

10 Conclusions

We have shown that the Laguerre expansion is a significant tool in the analysis of the QCD evolution equations from the numerical side. These advantages include both short running times in the actual implementation of the evolution and the possibility to have well defined recursion relations. The Laguerre algorithm is a very powerful way to address efficiently these problems.

We remark that polynomial expansions are going to be of wide use in the analysis of more general parton distributions -such as the non-forward or the double distributions- which have been introduced in the recent literature on Compton processes. Here we have just began our tour on the analysis of QCD renormalization group equations and their solutions by finite step integrations. We hope to return to the study of the extension of these methods to the non-diagonal partonic evolution in the near future.

Acknowledgements

We are grateful to Gordon Ramsey for discussions and for clarifying to us the Furmanski-Petronzio algorithm, and to Lionel Gordon for discussions.

11 Appendix. List of all the NLO polarized kernels

The references for the unpolarized NLO kernels are [2, 3]. The longitudinally polarized kernels can be found either as anomalous dimensions or splitting functions in [13, 14] The Perturbative expansion of the kernels is

$$\Delta P_{ij}(x, \alpha_s) = \left(\frac{\alpha_s}{2\pi}\right) \Delta P_{ij}^{(0)}(x) + \left(\frac{\alpha_s}{2\pi}\right)^2 \Delta P_{ij}^{(1)}(x) + \dots \quad (3)$$

where ij are flavour indices. The non-singlet and the singlet polarized LO kernels, respectively, are given by

$$\begin{aligned} \Delta P_{NS}^{(0)}(x) &= P_{qq}^{(0)}(x) = C_F \left(\frac{2}{(1-x)_+} - 1 - x + \frac{3}{2} \delta(1-x) \right) \\ \Delta P_{qq}^{(0)}(x) &= \Delta P_{NS}^{(0)}(x) \\ \Delta P_{qg}^{(0)}(x) &= 2n_f T_R (2x-1) \\ \Delta P_{gq}^{(0)}(x) &= C_F (2-x) \\ \Delta P_{gg}^{(0)}(x) &= 2C_G \left(\frac{1}{(1-x)_+} - 2x + 1 \right) + \frac{\beta_0}{2} \delta(1-x). \end{aligned} \quad (4)$$

The "+" distributions are defined by

$$\int_0^1 dx \frac{f(x)}{(1-x)_+} = \int_0^1 dx \frac{f(x) - f(1)}{1-x}. \quad (5)$$

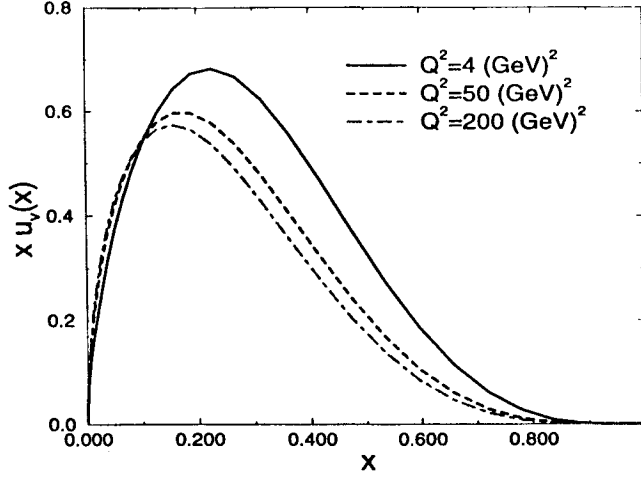


Figure 1: Unpolarized u_v is shown for various Q^2 values

The non-singlet NLO kernels are given by

$$\begin{aligned} \Delta P_{NS\pm}^{(1)} = & C_F^2 \left[P_F(x) \mp P_A(x) + \delta(1-x) \left(\frac{3}{8} - \frac{\pi^2}{2} + 6\zeta(3) \right) \right] \\ & + \frac{1}{2} C_F C_A \left[P_G(x) \pm P_A(x) + \delta(1-x) \left(\frac{17}{12} + \frac{11}{9} \pi^2 - 6\zeta(3) \right) \right] \\ & + C_F T_R n_f \left[P_{N_f}(x) - \delta(1-x) \left(\frac{1}{6} + \frac{2}{9} \pi^2 \right) \right] \end{aligned} \quad (6)$$

$$\begin{aligned} P_F(x) = & -2 \frac{1+x^2}{1-x} \ln x \ln(1-x) - \left(\frac{3}{1-x} + 2x \right) \ln x - \frac{1}{2} (1+x) \ln^2 x - 5(1-x) \\ P_A(x) = & 2 \left(\frac{1+x}{1+x^2} \right) S_2(x) + 2(1+x) \ln x + 4(1-x) \end{aligned}$$

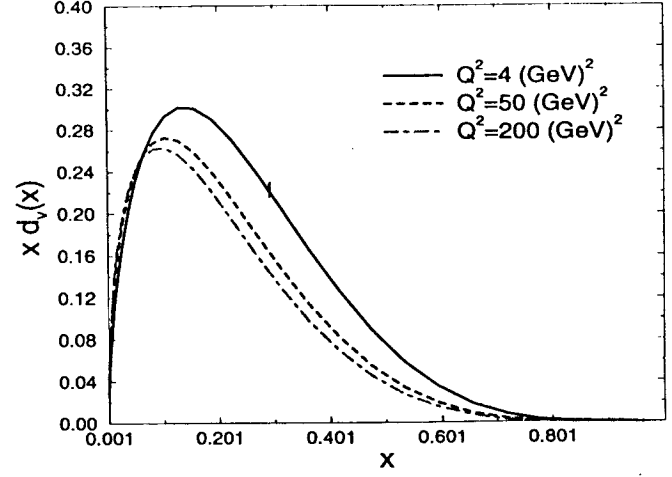


Figure 2: Unpolarized d_v is shown for various Q^2 values

$$\begin{aligned} P_G(x) = & \frac{1+x^2}{(1-x)_+} \left[\ln^2 x + \frac{11}{3} \ln x + \frac{67}{9} - \frac{\pi^2}{3} \right] + 2(1+x) \ln x + \frac{40}{3} (1-x) \\ P_{N_f}(x) = & \frac{2}{3} \left[\frac{1+x^2}{(1-x)_+} \left(-\ln x - \frac{5}{3} \right) - 2(1-x) \right] \end{aligned} \quad (7)$$

where

$$S_2(x) = -2Li_2(-x) - 2 \ln x \ln(1+x) + \frac{1}{2} \ln^2 x - \frac{\pi^2}{6}. \quad (8)$$

The NLO polarized singlet kernels are given by

$$\begin{aligned} \Delta P_{qq}^{(1)}(x) = & \Delta P_{NS\pm}^{(1)} + 2C_F T_R n_f \Delta F_{qq} \\ \Delta P_{qg}^{(1)}(x) = & C_F n_f T_R \Delta F_{qg}^{(1)}(x) + C_G n_f T_R \Delta F_{qg}^{(2)}(x) \end{aligned}$$

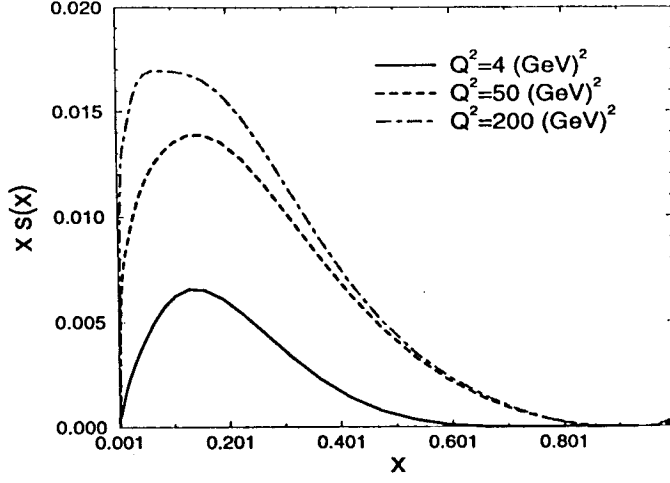


Figure 3: Unpolarized s is shown for various Q^2 values

$$\begin{aligned}\Delta F_{gg}^{(1)}(x) &= C_F n_f T_R \Delta F_{gg}^{(1)}(x) + C_F^2 F_{gg}^{(2)}(x) + C_F C_G \Delta F_{gg}^{(3)}(x) \\ \Delta P_{gg}^{(1)}(x) &= -C_G T_R n_f \Delta F_{gg}^{(1)}(x) - C_F T_R n_f \Delta F_{gg}^{(2)}(x) + C_G^2 \Delta F_{gg}^{(3)}(x)\end{aligned}\quad (9)$$

where $C_G = C_A = N_c$ and

$$\begin{aligned}\Delta F_{gg}(x) &= 1 - x - (1 - 3x) \ln x - (1 + x) \ln^2 x \\ \Delta F_{gg}^{(1)}(x) &= -22 + 27x - 9 \ln x + 8(1 - x) \ln(1 - x) \\ &\quad + \delta p_{gg}(x) \left[2 \ln^2 x (1 - x) - 4 \ln(1 - x) \ln x + \ln^2 x - \frac{2}{3} \pi^2 \right] \\ \Delta F_{gg}^{(2)}(x) &= 2(12 - 11x) - 8(1 - x) \ln(1 - x) + 2 \left(\frac{1}{3} + 8x \right) \ln x \\ &\quad - 2 \left[\ln^2(1 - x) - \frac{\pi^2}{6} \right] \delta p_{gg}(x) - [2S_2(x) - 3 \ln^2 x] \delta p_{gg}(-x) \\ \Delta F_{gg}^{(3)}(x) &= -\frac{4}{9}(x + 4) - \frac{4}{3} \delta p_{gg}(x) \ln(1 - x)\end{aligned}$$

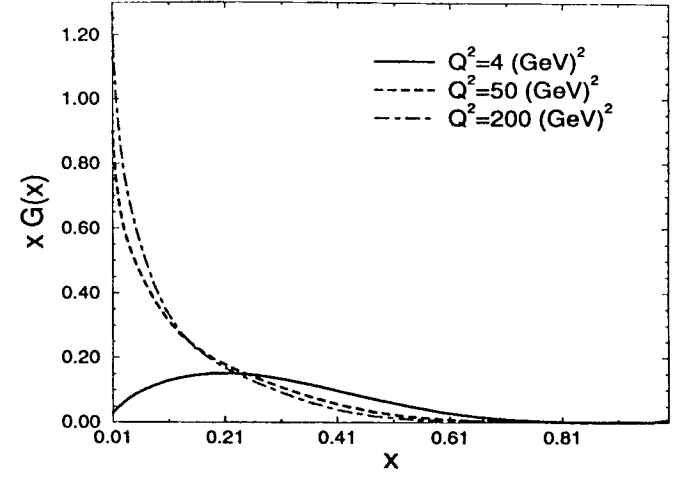


Figure 4: Unpolarized G is shown for various Q^2 values

$$\begin{aligned}\Delta F_{gg}^{(2)}(x) &= -\frac{1}{2} - \frac{1}{2}(4 - x) \ln x - \delta p_{gg}(-x) \ln(1 - x) + \left[-4 - \ln^2(1 - x) + \frac{1}{2} \ln^2 x \right] \delta p_{gg}(x) \\ \Delta F_{gg}^{(3)}(x) &= (4 - 13x) \ln x + \frac{1}{3}(10 + x) \ln(1 - x) + \frac{1}{9}(41 + 35x) + \frac{1}{2} [-2S_2(x) + 3 \ln^2 x] \delta p_{gg}(x) \\ &\quad + \left[\ln^2(1 - x) - 2 \ln(1 - x) \ln x - \frac{\pi^2}{6} \right] \delta p_{gg}(x) \\ \Delta F_{gg}^{(1)}(x) &= 4(1 - x) + \frac{4}{3}(1 + x) \ln x + \frac{20}{9} \delta p_{gg}(x) + \frac{4}{3} \delta(1 - x) \\ \Delta F_{gg}^{(2)} &= 10(1 - x) + 2(5 - x) \ln x + 2(1 + x) \ln^2 x + \delta(1 - x) \\ \Delta F_{gg}^{(3)}(x) &= \frac{1}{3}(29 - 67x) \ln x - \frac{19}{2}(1 - x) + 4(1 + x) \ln^2 x - 2S_2(x) \delta p_{gg}(-x) \\ &\quad + \left[\frac{67}{9} - 4 \ln(1 - x) \ln x + \ln^2 x - \frac{\pi^2}{3} \right] \delta p_{gg}(x) + \left[3\zeta(3) + \frac{81}{3} \right] \delta(1 - x),\end{aligned}$$

with

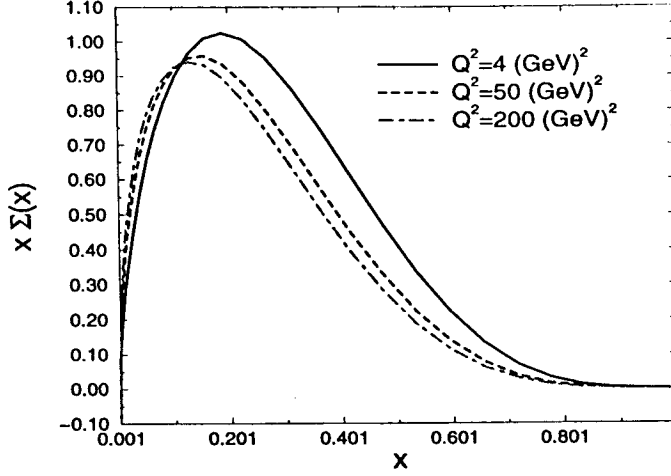


Figure 5: Unpolarized Σ is shown for various Q^2 values

$$\begin{aligned}
 \delta p_{qg}(x) &= 2x - 1 \\
 \delta p_{gq}(x) &= 2 - x \\
 \delta p_{gg}(x) &= \frac{1}{(1-x)_+} - 2x + 1.
 \end{aligned} \tag{11}$$

The unpolarized kernels, to LO are given by

$$P_{qq,NS}^{(0)} = \Delta P_{NS}^{(0)} \tag{12}$$

for the non-singlet sector, and by

$$\begin{aligned}
 P_{qq}^{(0)}(x) &= P_{qq,NS}^{(0)} \\
 P_{gg}^{(0)}(x) &= 2T_R n_f (x^2 + (1-x)^2)
 \end{aligned}$$

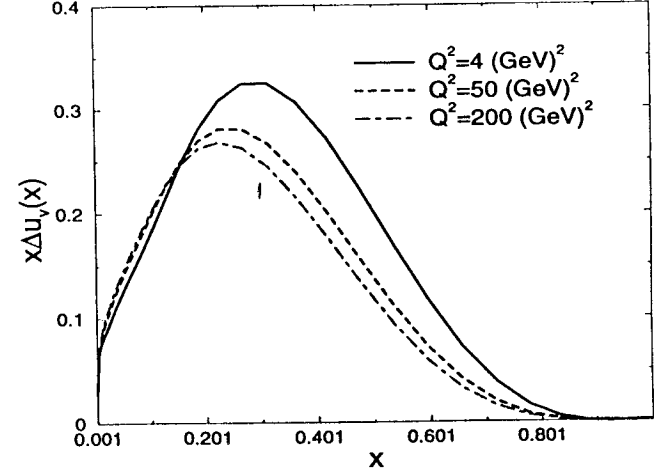


Figure 6: Longitudinally polarized u_v is shown for various Q^2 values

$$\begin{aligned}
 P_{gq}^{(0)}(x) &= C_F \frac{1 + (1-x)^2}{x} \\
 P_{gg}^{(0)}(x) &= 2N_c \left(\frac{1}{(1-x)_+} + \frac{1}{x} - 2 + x(1-x) \right) + \frac{\beta_0}{2} \delta(1-x)
 \end{aligned} \tag{13}$$

in the singlet sector.

The NLO unpolarized non-singlet and singlet kernels are given by

$$P_{NS}^{(1)\pm}(x) = \Delta P_{NS}^{(1)\mp}(x) \tag{14}$$

and

$$\begin{aligned}
 P_{qq}^{(1)}(x) &= P_{NS+}^{(1)} + 2C_F T_R n_f F_{qq} \\
 P_{qg}^{(1)}(x) &= C_F n_f T_R F_{qg}^{(1)}(x) + C_G n_f T_R \Delta F_{qg}^{(2)}(x) \\
 P_{gg}^{(1)}(x) &= C_F n_f T_R F_{gg}^{(1)}(x) + C_F^2 F_{gg}^{(2)}(x) + C_F C_G F_{gg}^{(3)}(x)
 \end{aligned}$$

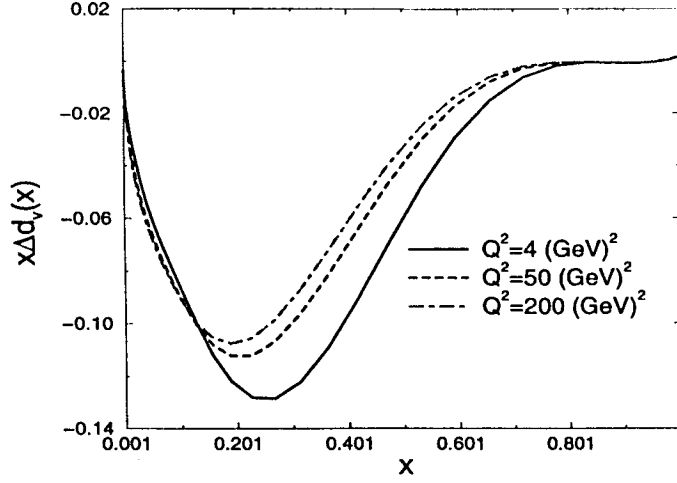


Figure 7: Longitudinally polarized d_v is shown for various Q^2 values

$$F_{gg}^{(1)}(x) = C_{FT_R} n_f F_{gg}^{(1)}(x) + C_{GT_R} n_f F_{gg}^{(2)}(x) + C_G^2 F_{gg}^{(3)}(x) \quad (15)$$

$$\begin{aligned} F_{qq}(x) &= \frac{20}{9x} - 2 + 6x - \frac{56}{9}x^2 + (1 + 5x + \frac{8}{3}x^2) \ln x - (1+x) \ln^2 x \\ F_{qq}^{(1)} &= 4 - 9x - (1-4x) \ln x - (1-2x) \ln^2 x + 4 \ln(1-x) \\ &+ \left[2 \ln^2 \left(\frac{1-x}{x} \right) - 4 \ln \left(\frac{1-x}{x} \right) - \frac{2}{3} \pi^2 + 10 \right] p_{qq}(x) \\ F_{gg}^{(2)} &= \frac{182}{9} + \frac{14}{9}x + \frac{40}{9x} + \left(\frac{136}{3}x - \frac{38}{3} \right) \ln x - 4 \ln(1-x) - (2+8x) \ln^2 x \\ &+ \left[-\ln^2 x + \frac{44}{3} \ln x - 2 \ln^2(1-x) + 4 \ln(1-x) + \frac{\pi^2}{3} - \frac{218}{9} \right] p_{qq}(x) \\ &+ 2p_{qq}(-x) S_2(x) \end{aligned}$$

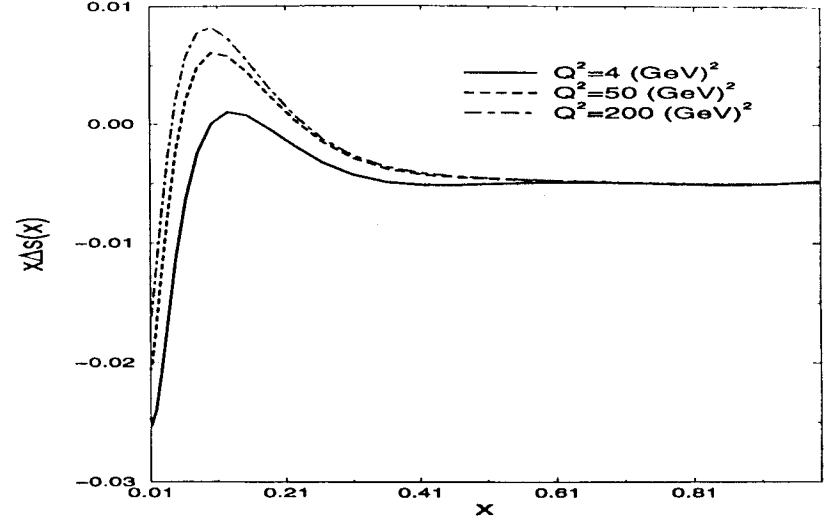


Figure 8: Longitudinally polarized s is shown for various Q^2 values

$$\begin{aligned} F_{qq}^{(1)} &= -\frac{4}{3}x - \left[\frac{20}{9} + \frac{4}{3} \ln(1-x) \right] p_{qq}(x) \\ F_{qq}^{(2)}(x) &= -\frac{5}{2} - \frac{7}{2}x + (2 + \frac{7}{2}x) \ln x - (1 - \frac{1}{2}x) \ln^2 x - 2x \ln(1-x) \\ &- \left[3 \ln(1-x) + \ln^2(1-x) \right] p_{qq}(x) \\ F_{qq}^{(3)}(x) &= \left(\frac{28}{9} + \frac{65}{18}x + \frac{44}{9}x^2 - (12 + 5x + \frac{8}{3}x^2) \ln x + (4+x) \ln^2 x + 2x \ln(1-x) \right. \\ &+ \left. \left[-2 \ln x \ln(1-x) + \frac{1}{2} \ln^2 x + \frac{11}{3} \ln(1-x) - \frac{\pi^2}{6} + \frac{1}{2} + \ln^2(1-x) \right] p_{qq}(x) \right. \\ &+ S_2(x) p_{qq}(-x) \\ F_{gg}^{(1)}(x) &= -16 + 8x + \frac{20}{3}x^2 + \frac{4}{3x} - (6 + 10x) \ln x - 2(1+x) \ln^2 x - \delta(1-x) \\ F_{gg}^{(2)}(x) &= 2 - 2x + \frac{26}{9}(x^2 - \frac{1}{x}) - \frac{4}{3}(1+x) \ln x - \frac{20}{9} p_{qq}(x) - \frac{4}{3} \delta(1-x) \end{aligned}$$

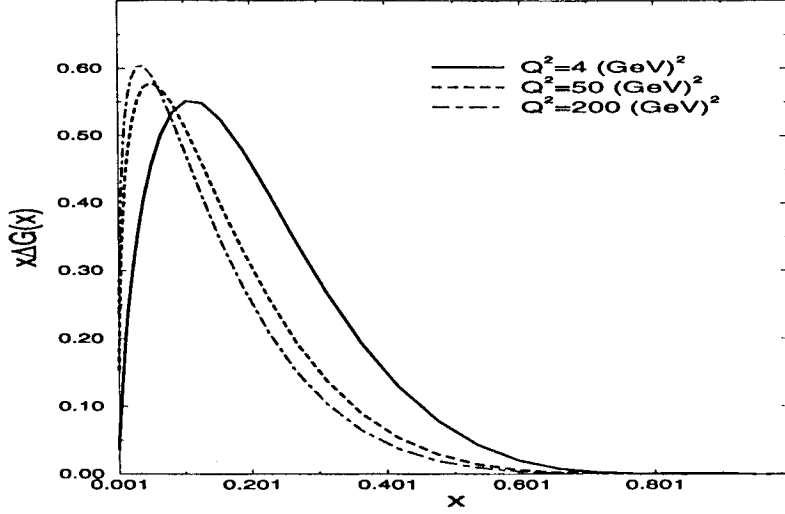


Figure 9: Longitudinally polarized G is shown for various Q^2 values

$$\begin{aligned}
 F_{gg}^{(3)}(x) = & \frac{27}{2}(1-x) + \frac{67}{9}\left(x^2 - \frac{1}{x}\right) - \left(\frac{25}{3} - \frac{11}{3}x + \frac{44}{3}x^2\right) \ln x + 4(1+x) \ln^2 x \\
 & + \left[\frac{67}{9} - 4 \ln x \ln(1-x) + \ln^2 x - \frac{\pi^2}{3}\right] p_{gg}(x) + 2p_{gg}(-x)S_2(x) \\
 & + \delta(1-x) \left(\frac{8}{3} + 3\zeta(3)\right)
 \end{aligned} \tag{16}$$

We have set

$$\begin{aligned}
 p_{qq}(x) &= \frac{2}{(1-x)_+} - 1 - x \\
 p_{gg}(x) &= x^2 + (1-x)^2 \\
 p_{gq}(x) &= \frac{1 + (1-x)^2}{x} \\
 p_{qg}(x) &= \frac{1}{(1-x)_+} + \frac{1}{x} - 2 + x(1-x)
 \end{aligned} \tag{17}$$

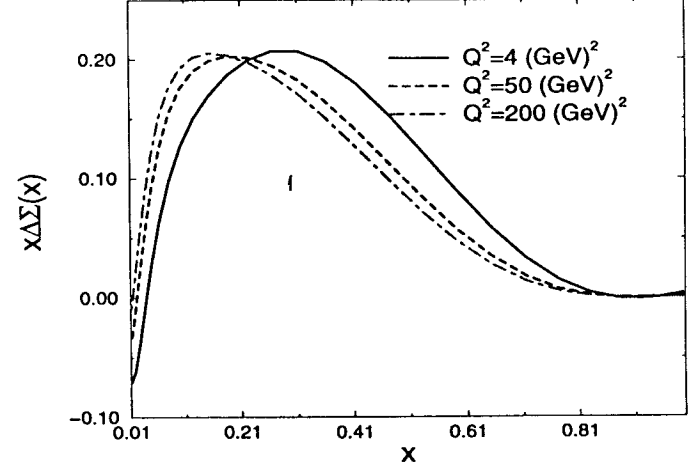


Figure 10: Longitudinally polarized Σ is shown for various Q^2 values

The kernel for the transverse polarization is written as

$$\Delta_T P_{q\pm} = \Delta_T P_{qq}^{(0)}(x) + \frac{\alpha_s(Q^2)}{2\pi} \Delta_T P_{q\pm}^{(1)}(x) \tag{18}$$

with the LO expression [16]

$$\Delta_T P_{q\pm} = C_F \left[\frac{2x}{(1-x)_+} + \frac{3}{2} \delta(1-x) \right]. \tag{19}$$

The NLO corrections are given by [17]

$$\begin{aligned}
 \Delta_T P_{q(\pm)}^{(1)}(x) &= \Delta_T P_{qq}^{(1)}(x) \pm \Delta_T P_{q\bar{q}}^{(1)}(x), \\
 \Delta_T P_{qq}^{(1)}(x) &= C_F^2 \left[1 - x - \left(\frac{3}{2} + 2 \ln(1-x)\right) \ln x \Delta_T P_{qq}^{(0)}(x) \right]
 \end{aligned}$$

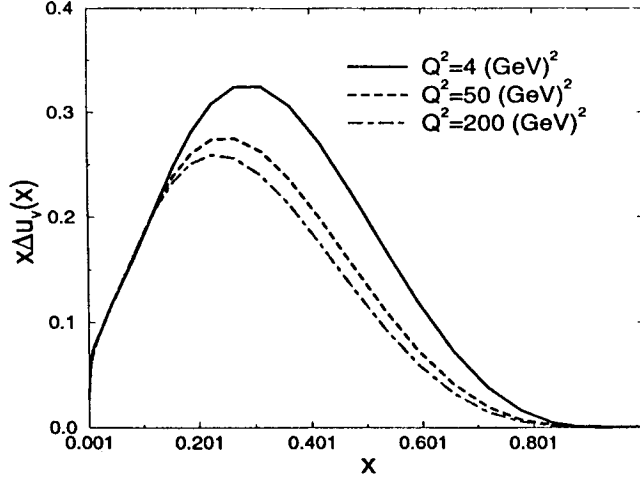


Figure 11: Transversely polarized u_v is shown for various Q^2 values

$$\begin{aligned}
& + \left(\frac{3}{8} - \frac{\pi^2}{2} + 6\zeta(3) \right) \delta(1-x) \Big] + \frac{1}{2} C_F C_G \left[-(1-x) + \left(\frac{67}{9} + \frac{11}{3} \ln x + \ln^2 x - \frac{\pi^2}{3} \right) \delta_T P_{qq}^{(0)}(x) \right. \\
& \left. + \left(\frac{17}{12} + \frac{11}{9} \pi^2 - 6\zeta(3) \right) \delta(1-x) \right] + \frac{2}{3} C_F T_{Rn_f} \left[\left(-\ln x - \frac{5}{3} \right) \delta_T P_{qq}^{(0)}(x) - \left(\frac{1}{4} + \frac{\pi^2}{3} \right) \delta(1-x) \right], \quad (21)
\end{aligned}$$

$$\Delta_T P_{qq}^{(1)}(x) = C_F \left(C_F - \frac{1}{2} C_G \right) \left(-(1-x) + 2S_2(x) \delta_T P^{(0)}(-x) \right). \quad (22)$$

References

- [1] G.P. Ramsey, Prog. Part. Nucl. Phys. 39 (1997) 599.
[2] W. Furmanski and R. Petronzio, Nucl. Phys. B195 (1982) 237;

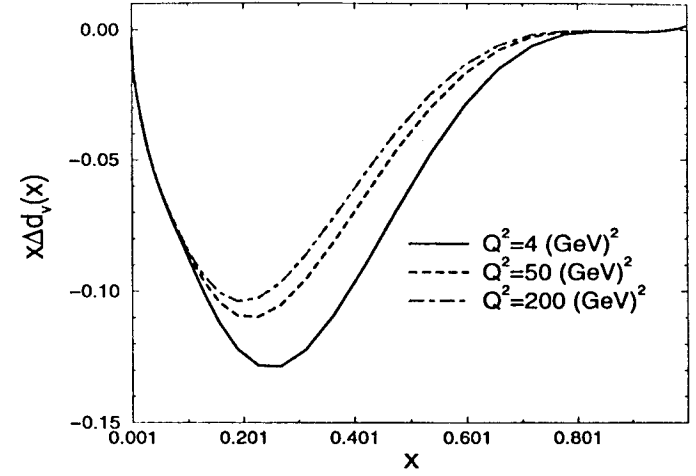


Figure 12: Transversely polarized d_v is shown for various Q^2 values

- [3] Z. Phys. C11 (1982) 293; Phys. Lett. 97B, (1980) 437.
[4] Notice that eqs. (3.26) and (3.37) of [2] should read as in our eq. (26) and eq. (36) respectively.
[5] M. Ropele, M. Traini and V. Vento, Nucl. Phys. A584 (1995) 634.
[6] X. Song, J.S. McCarthy and H.J. Weber, hep/ph 9702363. H. Weber X. Song and M. Kirchbach, Mod. Phys. Lett. A12, (1997) 729.
[7] N. Isgur and G. Karl, Phys. Rev. D 18 (1978) 4187; D19 (1979) 2653.
[8] A.V. Efremov and A.V. Radyushkin, Theor. Math. Phys. 42 (1980) 97; Phys. Lett. B94 (1980) 245; S.J. Brodsky and G.P. Lepage, Phys. Lett. B 87 (1979) 359; Phys. Rev. D22 (1980) 2157.
[9] X. Ji, Phys. Rev. D55 (1997) 7114; A.V. Radyushkin Phys. Rev. D56 (1997).

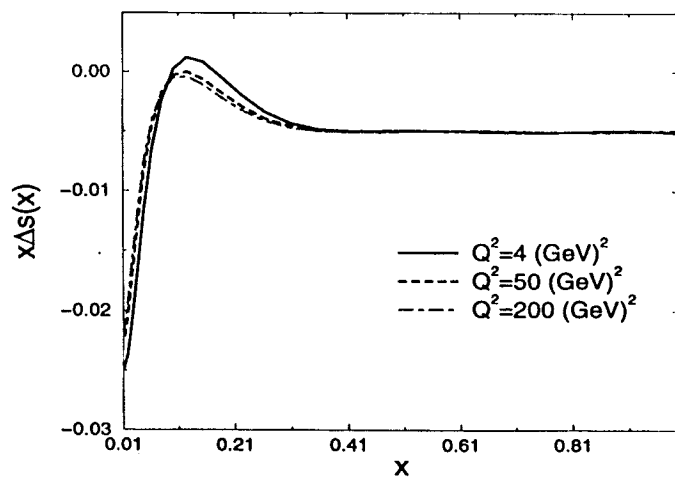


Figure 13: Transversely polarized s is shown for various Q^2 values

- [10] M. Hirai, S. Kumano, M. Miyama, *Comput.Phys.Commun.*108 (1998) 38; J. Blümlein, B. Geyer and D. Robaschik, *hep-ph/9711405*. M. Miyama, S. Kumano, *hep-ph/9508246*.
- [11] R. Kobayashi, M. Konuma, S. Kumano, *Comput.Phys.Commun.*86:264-278,1995.
- [12] G. Curci, W. Furmanski and R. Petronzio, *Nucl. Phys.* B175 (1980) 27.
- [13] R. Mertig and W. L. Van Neerven, *Z.Phys.*C70:637-654,1996.
- [14] W. Vogelsang, *Nucl.Phys.*B475:47-72,1996.
- [15] S. Chang, C. Corianò, R. D. Field and L. E. Gordon, *hep-ph/9705249*, to appear on *Nucl. Phys. B*; *Phys. Lett.* B403 (1997) 344.
- [16] X. Artru and M. Mekhfi, *Z. Phys.* C45 (1990) 669.

- [17] S. Kumano and M Miyama, *Phys. Rev.* D56 (1997) 2504; A. Hayashigaki, Y. Kanazawa and Y. Koike, *hep-ph/9707208*; W. Vogelsang, *hep-ph/9706511*.
- [18] G. Ramsey, *Journ. of Comput. Phys.* 60, (1985) 119.
- [19] S. Cotanch, unpublished.
- [20] T. Gehrmann and W.J. Sterling, *Z.Phys.*C65:461-470,1995.
- [21] D. Heddle, Y. R. Kwon and F. Tabakin, *Comp. Phys. Comm.* 38 (1985) 71.
- [22] Y.R. Kwon, F. Tabakin, *Phys. Rev. C* 18 (1978) 932.
- [23] J.P. Ralston and D.E. Soper, *Nucl. Phys.* B152 (1979) 109.
- [24] R.L. Jaffe and X. Ji, *Phys. Rev. Lett.* 67 (1991) 552;
- [25] H.L. Lai et al, *Phys. Rev.* D55, (1997) 1280; *Phys. Rev.* D51 (1996) 4763; W.K. Tung *hep-ph/9608293*.